Journal of Alloys and Compounds 688 (2016) 235–241

Contents lists available at ScienceDirect

Journal of Alloys and Compounds

journal homepage: http://www.elsevier.com/locate/jalcom

Non-hydrolytic sol-gel processing of chloride precursors loaded at forsterite stoichiometry

S. Rastegari [a], O. Seyed Mehdi Kani [a], E. Salahinejad [a, *], S. Fadavi [a], N. Eftekhari [a], A. Nozariasbmarz [b], L. Tayebi [c, d], D. Vashaee [b]

[a] Faculty of Materials Science and Engineering, K.N. Toosi University of Technology, Tehran, Iran
[b] Electrical and Computer Engineering Department, North Carolina State University, Raleigh, NC 27606, USA
[c] Department of Developmental Sciences, Marquette University School of Dentistry, Milwaukee, WI 53233, USA
[d] Department of Engineering Science, University of Oxford, Oxford OX1 3PJ, UK

ARTICLE INFO

Article history:
Received 11 April 2016
Received in revised form
30 June 2016
Accepted 18 July 2016
Available online 19 July 2016

Keywords:
Ceramics
Nanostructured materials
Sol-gel processes
Chemical synthesis

ABSTRACT

This paper for the first time investigates the sol-gel reaction of magnesium chloride and silicon tetrachloride, directed at the forsterite (Mg_2SiO_4) stoichiometry, using dry ethanol and glacial acetic acid as the solvent and chelating agent, respectively. The synthesized particles before and after calcination were characterized by transmission electron microscopy equipped with energy-dispersive X-ray spectroscopy mapping, X-ray diffraction and Fourier transform infrared spectroscopy. According to the results, the calcined nanoparticles showed a magnesia/forsterite structure along with silicon depletion, despite loading the forsterite stoichiometry. On the other hand, silicon-acetoxy bonds were detected in the xerogel (before calcination) as a result of the chelation reaction, albeit with a relatively uniform distribution of the essential elements. Since no non-alcoholyzed silicon-chlorine bond was detected in the xerogel, the development of the calcined structure was explained by the deficient sol-gel condensation and subsequent evaporation of silicon tetraacetate. It was inferred that the excessive amount of hydrogen chloride as the coproduct of the ethanolysis and chelation reactions of the precursors inhibits the condensation step, as confirmed by a supplementary test in an exaggerated circumstance. In conclusion, the silicon-containing species acts like a limiting reagent in the sol-gel condensation of forsterite using the chloride precursors and acetic acid chelator, in spite of loading the related stoichiometry.
© 2016 Elsevier B.V. All rights reserved.

1. Introduction

Forsterite is a magnesium silicate with the chemical formula Mg_2SiO_4 and orthorhombic crystal structure. This ceramic has a low electrical conductivity and high melting point (1890 °C), which makes it a suitable material for electrical insulation even at high temperatures. Also, it has good refractory properties for high-temperature applications, due to its high melting point, low thermal expansion, elevated chemical stability, and great insulation properties [1]. From the biomedical viewpoint, forsterite contains ions that are released in biological environments, leading to the development of a hydroxy-carbonate apatite layer with a positive effect on bone calcification. Moreover, forsterite shows good biocompatibility, bioactivity, biodegradability and, more importantly, improved mechanical properties (fracture toughness) compared to hydroxyapatite [2]. In this regard, nanocrystalline forsterite has superior mechanical and bioactivity behaviors compared with coarse-sized forsterite [3,4]. Among the methods developed for the synthesis of nanocrystalline forsterite, the sol-gel process provides a highly homogeneous mixture of initial components, reduced crystallization temperature, and controllable morphology and phase composition, due to molecular-level mixing of the precursors.

There are a number of reports in the literature on the sol-gel synthesis of forsterite, where most of them have used tetraethyl orthosilicate (TEOS) as the silicon precursor and salts like $Mg(NO_3)_2$, $Mg(CH_3COO)_2$, and $Mg(OCH_3)_2$ as the magnesium source. In the sol-gel synthesis of multi-component silicate systems, the different rates of hydrolysis and condensation between/among precursors pose a challenge. This can result in a chemical inhomogeneity of the gel, leading to a higher crystallization

* Corresponding author.
E-mail addresses: salahinejad@kntu.ac.ir, erfan.salahinejad@gmail.com (E. Salahinejad).

http://dx.doi.org/10.1016/j.jallcom.2016.07.187
0925-8388/© 2016 Elsevier B.V. All rights reserved.

temperature and undesirable phases. Several approaches have been used to overcome this limitation, such as a slow addition of water, partial pre-hydrolysis of silicon alkoxides, and chemical modification by chelating agents [5]. Among them, ethanolic sol-gel processing of TEOS with magnesium methoxide, acetate or nitrate precursors using acetic acid as the chelating agent is known as a routine procedure for forsterite synthesis [5–9]. Nevertheless, the type of sol-gel precursors is a variable affecting the product characteristics. Despite the lower cost and more gelation rate of silicon tetrachloride ($SiCl_4$) compared to TEOS [10], to our knowledge, little work has been focused on using $SiCl_4$ as the silicon source to synthesize multi-component silicates. Alternatively, chloride precursors have been successfully used to synthesize other multi-component ceramics, for example zirconium titanate [11–20]. This work aims to study the non-hydrolytic sol-gel reaction of magnesium chloride and silicon tetrachloride loaded at the forsterite stoichiometry using ethanol as the solvent and acetic acid as the chelating agent, for the first time.

2. Experimental procedure

The used processing procedure was similar to that reported in Refs. [5–9] in which albeit TEOS and magnesium methoxide ($Mg(OCH_3)_2$) were precursors. However, in the current work, other precursors (chlorides) as a sol-gel variable were tested. Anhydrous magnesium chloride ($MgCl_2$, Merck, Germany, >98%), silicon tetrachloride ($SiCl_4$, Merck, Germany, >99%), dry ethanol (C_2H_5OH, Merck, Germany, 100%), and glacial acetic acid (CH_3COOH, Merck, Germany, 100%) were used as starting materials. Typically, 1.6 gr $MgCl_2$ was dissolved in 30 ml ethanol and 2 ml acetic acid by using a magnetic stirrer. After complete dissolution, the proper amount of $SiCl_4$ (the molar ratio of Si:Mg was 1:2 based on the forsterite stoichiometry) was introduced dropwise to the above solution and stirred for 2 h. The resultant clear sol was aged at room temperature for 48 h and then dried at 80 °C for 6 h, giving a white xerogel. Afterward, an amount of the obtained xerogel was calcined at 800 °C for 2 h to proceed crystallization and develop forsterite. Additionally, in order to confirm the justification presented for the above calcined structure, a new sample was synthesized similar to the above procedure, only with this difference that 60 μL hydrochloric acid solution (HCl, Merck, Germany, 37%) was added to the sol as well as the acetic acid addition.

The xerogel and calcined powders were characterized by transmission electron microscopy equipped with energy-dispersive X-ray spectroscopy mapping (TEM/XMAP, FEI Titan 80-300, 200 kV), X-ray diffraction (XRD, Bruker AXS, Cu Kα radiation) and Fourier transform infrared spectroscopy (FTIR, Bruker Vector 22). For the TEM studies, a small content of the samples was dispersed in water, ultrasonicated for 10 min and then dropped on a copper grid. For the powder XRD analysis, a scan step size of 0.02° and scan step time of 4 s were used. Also, a wavenumber range of 500–4000 cm^{-1} with a resolution of 2 cm^{-1} was used for the FTIR experiments.

3. Results and discussion

Fig. 1a and b shows the TEM micrograph of the xerogel powder synthesized without the HCl solution, where both bright-field and dark-field images were represented for a better contrast and easier recognition. As can be seen, the xerogel is composed of nanoparticles with a relatively irregular shape, a size distribution of 10–50 nm, and a mean size of 20 nm. Since the sol-gel process is conducted at a liquid phase and low temperature, ionic rearrangements required to obtain stable crystalline phases do not occur during processing. Thus, sol-gel derived products generally

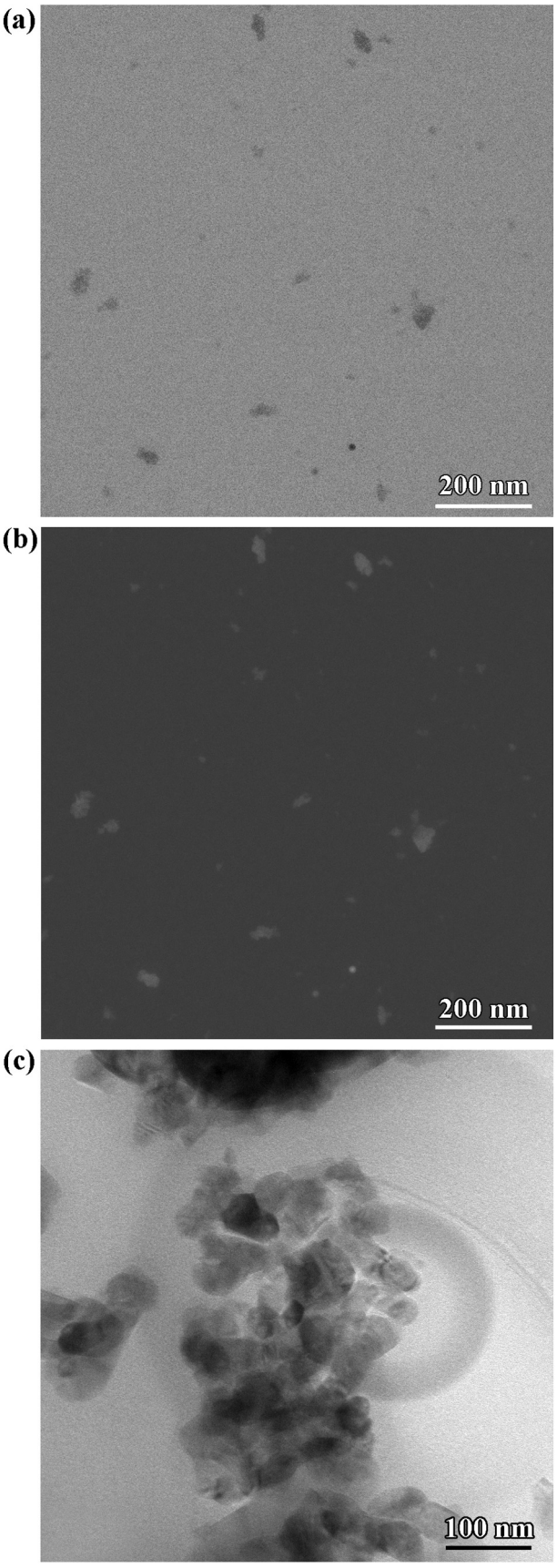

Fig. 1. TEM micrograph of the xerogel powder synthesized without the HCl addition: bright-field (a) and dark-field (b), and the powder calcined at 800 °C for 2 h (c).

have metastable amorphous structures [21] and a calcination process is normally followed to achieve thermodynamically stable structures. The TEM micrograph of the related powder after calcination at 800 °C is also depicted in Fig. 1c. As can be seen, the nanoparticles have experienced the coarsening phenomenon with a size distribution of 20–80 nm and mean size of 50 nm, to decrease the surface energy. Also, to again decrease the global surface energy via evaporation-condensation and surface diffusion mechanisms [22], the particle curvature has been reduced and the surfaces have tended to be flat, i.e. nanoparticle rounding.

Considering the fact that the silicon and magnesium precursors were loaded at the forsterite stoichiometry (the molar ratio of $SiCl_4$:$MgCl_2$ was 1:2), a fully forsterite structure was anticipated after calcination. The XRD pattern of the powder calcined at 800 °C is demonstrated in Fig. 2. As can be seen, as well as forsterite, a considerable amount of magnesia (MgO) is detected in the XRD data, despite the fact that this procedure has resulted in the development of a fully forsterite structure albeit while using other precursors [5–9]. To realize the origin of this unexpected structure, supplementary analyses including XMAP and FTIR were carried out on the xerogel and calcined powders, as follows.

Fig. 3 indicates XMAP of Si, Mg, O, and Cl for the xerogel, where a large particle was selected to record strong X-ray signals. In this sample, a relatively uniform distribution of the elements is observed, which is a desirable feature. However, according to Fig. 4 showing XMAPs for the calcined powder, regarding the principal elements of Si, Mg, and O forming forsterite, silicon depletion is observed. This is in agreement with the XRD result of the calcined powder, so that there has not been enough silicon for the transformation of retained magnesia to forsterite. This suggests that some silicon-containing species in the xerogel, despite detected in the related XMAP, are not involved in the oxide network. Instead, they take part in volatile compounds which evaporate during calcination, leading to silicon depletion and thereby the silicon lack to form a fully forsterite structure in the calcined sample. Since XMAP essentially is an elemental analysis method and cannot give information about bonds, spectroscopic analyses can be useful to identify silicon bonds. Albeit, considering the fact that the calcined sample is composed of forsterite and magnesia (Fig. 2), the type of its bonds is ultimately known. However, the identification of bonds in the amorphous xerogel cannot be done by XRD and was alternatively conducted by the FTIR approach.

Fig. 5 represents the FTIR spectra of the xerogel and calcined powder samples. In the xerogel, the bands centered at about 3500 and 3332 cm^{-1} belong to O–H stretching (ethanol) [23]. Also, the sharp peak at 1608 cm^{-1} is attributed to HCl [24], as a coproduct as the coproduct of the ethanolysis and chelation reactions of the used chloride precursors, so that its considerable intensity suggests its significant concentration in the sol and xerogel. The band at about 1050 cm^{-1} is also related to C–O symmetric stretching (ethanol) [23]. These four peaks clearly disappeared in the calcined spectrum because of evaporation during heating, considering the low boiling point of these compounds. Concerning the Mg component, the band around 549 cm^{-1} is attributed to the vibration of MgO_4 tetrahedral in a silicate network [5–9,25]. The intensity of this peak in the calcined sample is lower than the xerogel. In return, in the calcined spectrum, another peak exists at 586 cm^{-1} belonging to a Mg–O vibration (magnesia) [26], which is in good agreement with the presence of magnesia in the calcined sample based on the XRD analysis (Fig. 2). In the calcined sample, the bands centered at about 873 and 1000 cm^{-1} correspond to SiO_4 stretching in forsterite [6], confirming the XRD result. With regard to silicon-containing species, the band at 850 cm^{-1} is related to a Si–OH stretching vibration [5–9,27], which is another indicative of the sol-gel alcoholysis of silicon tetrachloride. Note that this type of alcoholysis is beneficial to have a desirable forsterite structure after calcination, because it cannot evaporate during calcination and cause the detected silicon depletion. Nonetheless, the key point drawn from the FTIR analyses is related to Si-containing bonds which exist in the xerogel, but do not exist in the calcined sample due to the evaporation loss. In this regard, the bands centered at about 945 and 1250 cm^{-1} belongs to acetoxy groups (CH_3COO–) attached to silicon [28] (typically silicon tetraacetate) in the xerogel sample, as formed by the reaction of silicon tetrachloride and acetic acid (chelation reaction). The absence of these vibrations in the calcined sample infers its evaporation during calcination.

Apart from silicon tetraacetate, the probable presence of other low boiling-point silicon-containing compounds in the xerogel and their subsequent evaporation during calcination should be checked. First, the hypothesis of the formation of TEOS through ethanolysis of silicon tetrachloride (based on Eq. (1)) is rejected, due to the absence of its vibrations in the FTIR spectra.

$$SiCl_4 + 4C_2H_5OH = Si(OC_2H_5)_4 + 4HCl \quad (1)$$

The second possible compound is non-alcoholyzed silicon tetrachloride as another low boiling-point species, i.e. the hypothesis of the incomplete alcoholysis of this precursor. This assumption is also rejected, although vibration bands belonging to Si–Cl essentially locate in the range of 500–625 cm^{-1} [28]. Because these

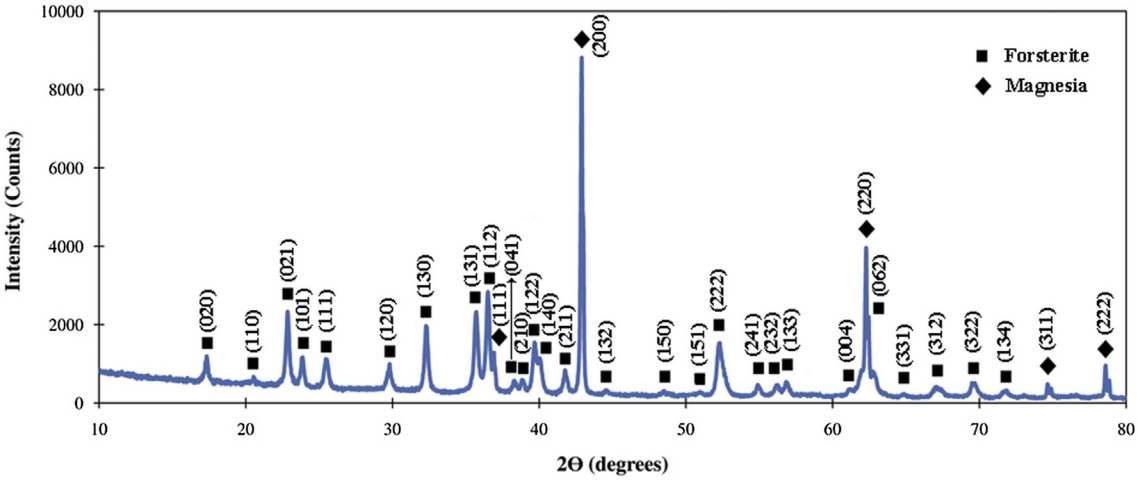

Fig. 2. XRD pattern of the powder calcined at 800 °C for 2 h (without the HCl addition).

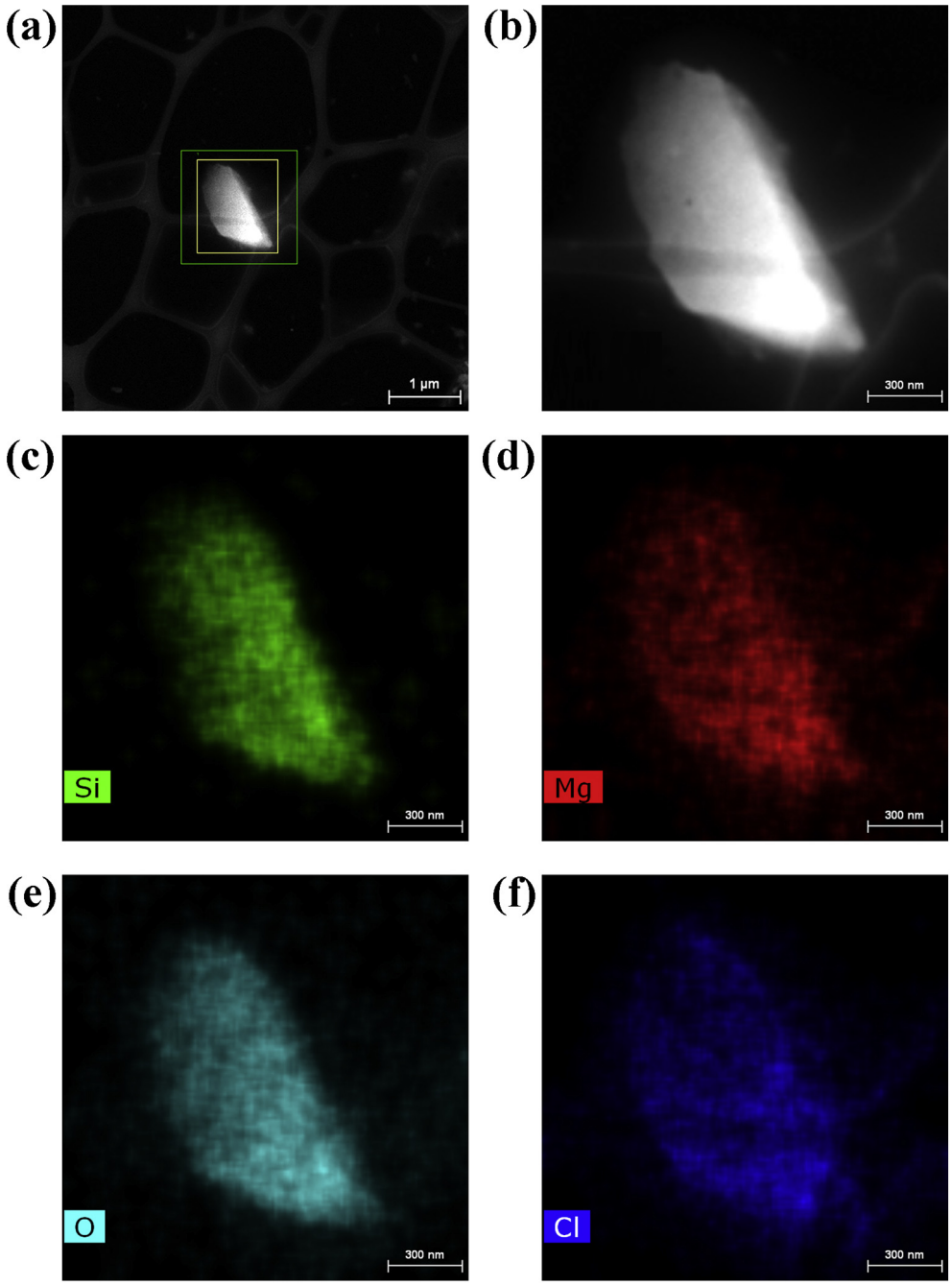

Fig. 3. TEM micrograph of the xerogel powder synthesized without the HCl addition in two magnifications (a and b) and XMAP of Si (c), Mg (d), O (e), and Cl (f).

vibrations cannot exist in the calcined sample due to evaporation, and there is no extra peak in this wavenumber range of the xerogel spectrum compared to the calcined one. Thus, the only volatile compound in the xerogel is silicon tetraacetate. In other words, the imperfect sol-gel reaction developing the non-stoichiometric calcined product is merely related to the condensation step since non-alcoholyzed Si–Cl vibrations were not detected in the xerogel.

Indeed, silicon tetraacetate is formed during the mixing process in the solution, based on Eq. (2) (chelation reaction).

$$SiCl_4 + 4CH_3COOH = Si(OCOCH_3)_4 + 4HCl \quad (2)$$

However, this compound could not be effectively condensed and thereby participate in the oxide network during the employed sol-gel process. Alternatively, it would evaporate during calcination, resulting in the silicon depletion and lack to form a fully forsterite structure in the calcined sample. The question that arises is why the sol-gel condensation of silicon tetraacetate is inhibited. In previous studies [5–9], while using other precursors and acetic acid as the chelating agent, polycondensation has been completely conducted, leading to the desirable forsterite structure. The main difference is related to the chloride precursors used in this work, where a significant amount of HCl is released from the alcoholysis and chelation reactions, as implied by its strong infrared peak in the xerogel. Indeed, the excessive content of this compound in this employed sol-gel method disturbs polycondensation required for the complete sol-gel reaction and development of forsterite. It is noteworthy that the trace addition of acids like HCl beneficially affects

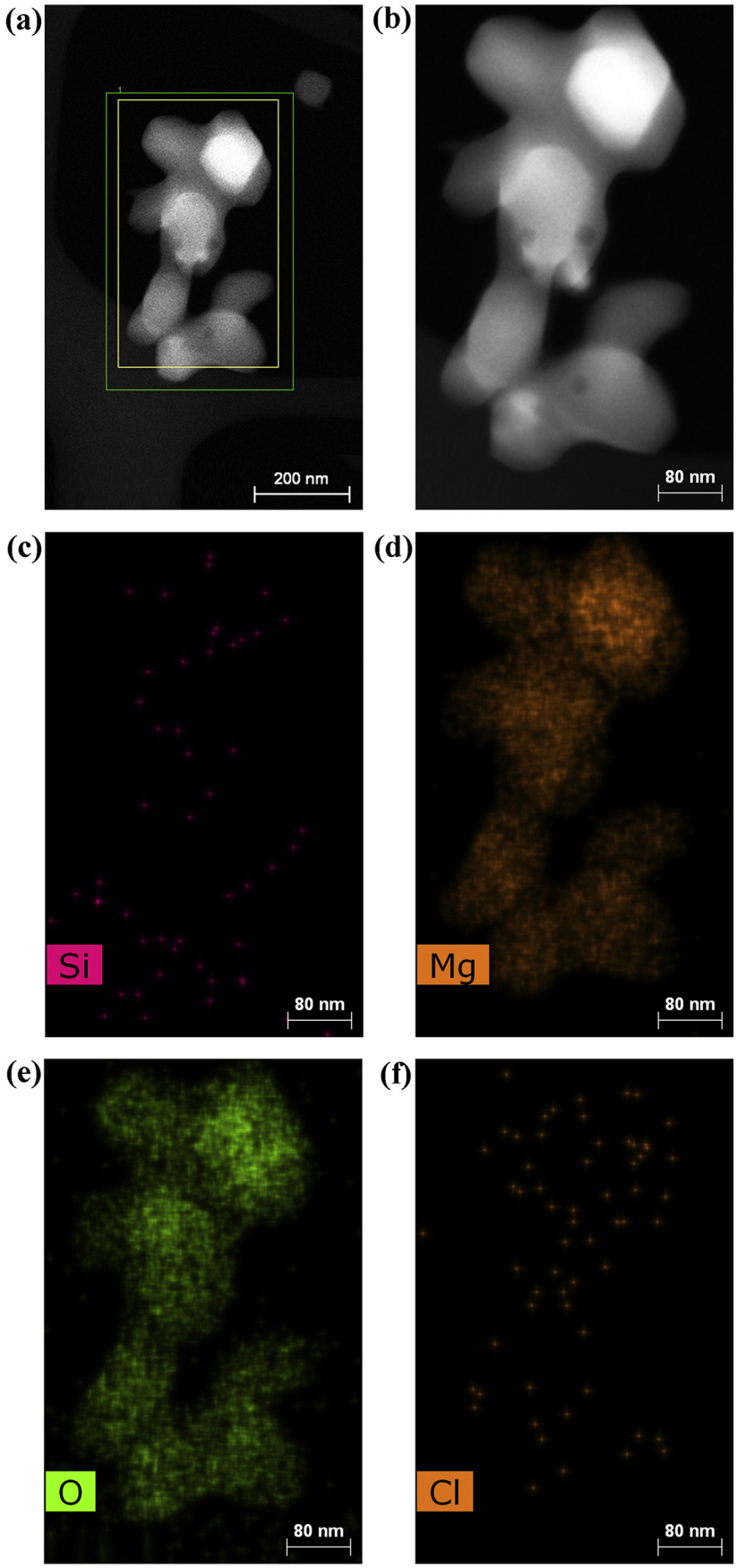

Fig. 4. TEM micrograph of the calcined powder (without the HCl addition) in two magnifications (a and b) and XMAP of Si (c), Mg (d), O (e), and Cl (f).

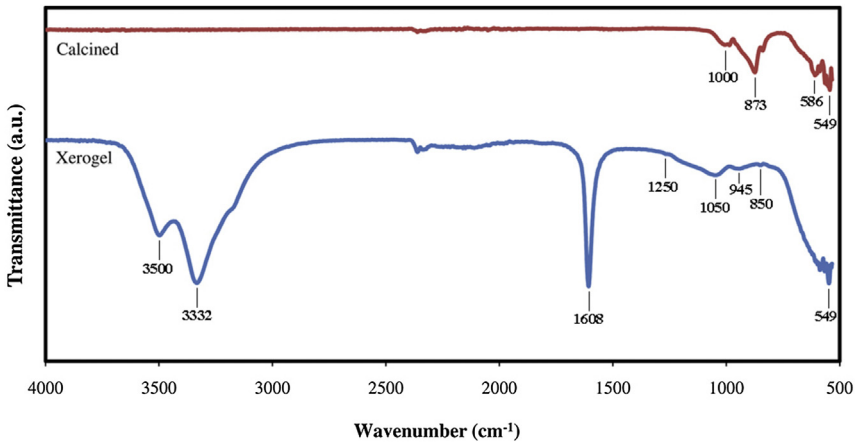

Fig. 5. FTIR spectra of the xerogel and calcined powder samples (without the HCl addition).

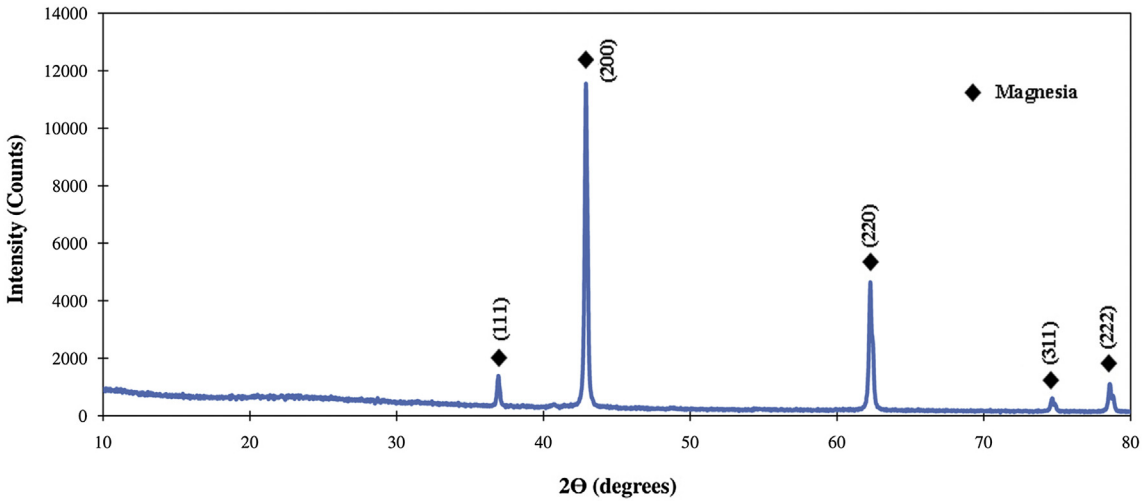

Fig. 6. XRD pattern of the sample synthesized with the HCl addition after calcination at 800 °C for 2 h.

the gelation reaction of silicon tetraacetate [29].

To confirm and highlight the inhibiting effect of excessive HCl on the aforementioned sol-gel condensation step, a new sample was synthesized similar to the above one, but with the HCl solution addition, as the exaggerated test. Fig. 6 shows the XRD pattern of this sample after calcination. As can be seen, the intensity of the magnesia reflections has been increased and, more importantly, the forsterite peaks have disappeared in comparison to Fig. 2, suggesting a more silicon depletion and lack. Considering the promoting role of water in both hydrolysis and condensation sol-gel reactions [30,31], even with the presence of water in the HCl solution used for this exaggerated sample, any improvement in the expected calcined structure was not only achieved, but also the deviation with respect to the expected stoichiometry was enhanced. It suggests the domination of the inhibiting role of HCl and verifies the above described mechanism about condensation inhibited by the severe chelation effect.

In conclusion, this employed sol-gel procedure, which was similar to the common methods of synthesizing forsterite albeit from other precursors, cannot direct the synchronous polycondensation of the used chloride precursors, due to condensation inhibited by the excessive amount of HCl. Thus, the silicon-containing species acts like a limiting reagent in the sol-gel condensation of forsterite using the chloride precursors and acetic acid chelator, in spite of loading the related stoichiometry.

4. Conclusions

A non-hydrolytic sol-gel process using $MgCl_2$ and $SiCl_4$ as the precursors, ethanol as the solvent, and acetic acid as the chelating agent was structurally investigated. Both the obtained xerogel (dried alcohogel) and calcined powder particles were nanometric in size, where calcination was performed at 800 °C for 2 h. The calcined powder displayed a forsterite/magnesia composite structure with a silicon depletion, despite loading the precursors at the forsterite stoichiometry. Silicon-acetoxy bonds were detected in the xerogel sample, with a relatively uniform distribution of the elements. During heating, the evaporation of these non-polycondensed silicon tetraacetate molecules caused the silicon depletion and justified the unexpected calcined structure. The inhibiting role of excessive HCl in the polycondensation reaction was also confirmed by the exaggerated experiment.

Acknowledgements

The work at NCSU was partially based upon work supported by AFOSR under contract number FA9550-12-1-0225 and NSF under grant numbers EEC-1160483, ECCS-1351533 and CMMI-1363485.

The work at MU was supported by NSF grant CMMI-1363485.

References

[1] M.B. Mitchell, D. Jackson, P.F. James, Preparation and characterisation of forsterite (Mg_2 SiO_4) aerogels, J. Non-Crystalline Solids 225 (1998) 125–129.

[2] S. Ramesh, A. Yaghoubi, K.S. Lee, K.C. Chin, J. Purbolaksono, M. Hamdi, M. Hassan, Nanocrystalline forsterite for biomedical applications: synthesis, microstructure and mechanical properties, J. Mech. Behav. Biomed. Mater. 25 (2013) 63–69.

[3] M. Kharaziha, M. Fathi, Improvement of mechanical properties and biocompatibility of forsterite bioceramic addressed to bone tissue engineering materials, J. Mech. Behav. Biomed. Mater. 3 (2010) 530–537.

[4] F. Tavangarian, R. Emadi, Nanostructure effects on the bioactivity of forsterite bioceramic, Mater. Lett. 65 (2011) 740–743.

[5] M. Tsai, Effects of hydrolysis processing on the character of forsterite gel fibers. Part II: crystallites and microstructural evolutions, J. Eur. Ceram. Soc. 22 (2002) 1085–1094.

[6] M.T. Tsai, Characterization of nanocrystalline forsterite fiber synthesized via the sol–gel process, J. Am. Ceram. Soc. 85 (2002) 453–458.

[7] M. Tsai, Effects of hydrolysis processing on the character of forsterite gel fibers. Part I: preparation, spinnability and molecular structure, J. Eur. Ceram. Soc. 22 (2002) 1073–1083.

[8] M. Tsai, Hydrolysis and condensation of forsterite precursor alkoxides: modification of the molecular gel structure by acetic acid, J. Non-Crystalline Solids 298 (2002) 116–130.

[9] M. Tsai, Synthesis of nanocrystalline forsterite fiber via a chemical route, Mater. Res. Bull. 37 (2002) 2213–2226.

[10] M.B. Mitchell, D. Jackson, P.F. James, Preparation of forsterite (Mg_2SiO_4) powders via an aqueous route using magnesium salts and silicon tetrachloride (SiCl4), J. Sol-gel Sci. Technol. 15 (1999) 211–219.

[11] E. Salahinejad, M. Hadianfard, D. Macdonald, I. Karimi, D. Vashaee, L. Tayebi, Aqueous sol–gel synthesis of zirconium titanate (ZrTiO 4) nanoparticles using chloride precursors, Ceram. Int. 38 (2012) 6145–6149.

[12] E. Salahinejad, M. Hadianfard, D. Macdonald, M. Mozafari, K. Walker, A.T. Rad, S. Madihally, D. Vashaee, L. Tayebi, Surface modification of stainless steel orthopedic implants by sol–gel ZrTiO4 and ZrTiO4–PMMA coatings, J. Biomed. Nanotechnol. 9 (2013) 1327–1335.

[13] M. Mozafari, E. Salahinejad, V. Shabafrooz, M. Yazdimamaghani, D. Vashaee, L. Tayebi, Multilayer bioactive glass/zirconium titanate thin films in bone tissue engineering and regenerative dentistry, Int. J. Nanomedicine 8 (2013) 1665–1672.

[14] P. Rouhani, E. Salahinejad, R. Kaul, D. Vashaee, L. Tayebi, Nanostructured zirconium titanate fibers prepared by particulate sol–gel and cellulose templating techniques, J. Alloys Compd. 568 (2013) 102–105.

[15] E. Salahinejad, M. Hadianfard, D. Macdonald, M. Mozafari, D. Vashaee, L. Tayebi, Multilayer zirconium titanate thin films prepared by a sol–gel deposition method, Ceram. Int. 39 (2013) 1271–1276.

[16] E. Salahinejad, M. Hadianfard, D. Macdonald, M. Mozafari, D. Vashaee, L. Tayebi, A new double-layer sol–gel coating to improve the corrosion resistance of a medical-grade stainless steel in a simulated body fluid, Mater. Lett. 97 (2013) 162–165.

[17] E. Salahinejad, M. Hadianfard, D. Macdonald, M. Mozafari, D. Vashaee, L. Tayebi, Zirconium titanate thin film prepared by an aqueous particulate sol–gel spin coating process using carboxymethyl cellulose as dispersant, Mater. Lett. 88 (2012) 5–8.

[18] E. Salahinejad, M. Hadianfard, D. Vashaee, L. Tayebi, Influence of annealing temperature on the structural and anti-corrosion characteristics of sol–gel derived, spin-coated thin films, Ceram. Int. 40 (2014) 2885–2890.

[19] E. Salahinejad, M. Hadianfard, D. Vashaee, L. Tayebi, Effect of precursor solution pH on the structural and crystallization characteristics of sol–gel derived nanoparticles, J. Alloys Compd. 589 (2014) 182–184.

[20] M. Mozafari, E. Salahinejad, S. Sharifi-Asl, D. Macdonald, D. Vashaee, L. Tayebi, Innovative surface modification of orthopaedic implants with positive effects on wettability and in vitro anti-corrosion performance, Surf. Eng. 30 (2014) 688–692.

[21] A.V. Vinogradov, V.V. Vinogradov, Low-temperature sol–gel synthesis of crystalline materials, RSC Adv. 4 (2014) 45903–45919.

[22] C.J. Brinker, G.W. Scherer, Sol-gel Science: the Physics and Chemistry of Sol-gel Processing, Academic press, 2013.

[23] F. Rubio, J. Rubio, J. Oteo, A FT-IR study of the hydrolysis of tetraethylorthosilicate (TEOS), Spectrosc. Lett. 31 (1998) 199–219.

[24] C.A. Kumar, J. Sreekanth, N. Raghunandan, Preparation and in-vitro evaluation of controlled release metformin hcl matrix tablet and immediate release pioglitazone hcl bilayer tablets for treatment for type-ii diabetes, Indo Am. J. Pharm. Res. 3 (2013) 1521–1529.

[25] D. Mazza, M. Lucco-Borlera, G. Busca, A. Delmastro, High-quartz solid-solution phases from xerogels with composition 2MgO. $2Al_2O_3$. $5SiO_2$ (μ-cordierite) and Li_2O. Al $_2O_3$. $nSiO_2$ (n= 2 to 4)(β-eucryptite): characterization by XRD, FTIR and surface measurements, J. Eur. Ceram. Soc. 11 (1993) 299–308.

[26] P. Tamilselvi, A. Yelilarasi, M. Hema, R. Anbarasan, Synthesis of hierarchical structured MgO by sol-gel method, Nano Bull. 2 (2013) 130106.

[27] M. Nogami, S. Ogawa, K. Nagasaka, Preparation of cordierite glass by the sol-gel process, J. Mater. Sci. 24 (1989) 4339–4342.

[28] P.J. Launer, Infrared analysis of organosilicon compounds: spectra-structure correlations, Silicone Compd. Register Rev. (1987) 100–103.

[29] B.K. Coltrain, L.W. Kelts, N.J. Armstrong, J.M. Salva, Silicon tetraacetate as a sol-gel precursor, J. Sol-Gel Sci. Technol. 3 (1994) 83–90.

[30] M. Tsai, Preparation and crystallization of forsterite fibrous gels, J. Eur. Ceram. Soc. 23 (2003) 1283–1291.

[31] G. Afonina, V. Leonov, O. Popova, Effect of the conditions of hydrolysis of tetraethoxysilane on the synthesis of forsterite, Glass Ceram. 65 (2008) 447–451.